



AFRL-RX-WP-TP-2011-4362

**FATIGUE CRACK DETECTION VIA LOAD-
DIFFERENTIAL GUIDED WAVE METHODS (PREPRINT)**

Jennifer E. Michaels, Sang Jun Lee, Xin Chen, and Thomas E. Michaels

Georgia Tech Research Group

NOVEMBER 2011

Approved for public release; distribution unlimited.

See additional restrictions described on inside pages

STINFO COPY

**AIR FORCE RESEARCH LABORATORY
MATERIALS AND MANUFACTURING DIRECTORATE
WRIGHT-PATTERSON AIR FORCE BASE, OH 45433-7750
AIR FORCE MATERIEL COMMAND
UNITED STATES AIR FORCE**

REPORT DOCUMENTATION PAGE				<i>Form Approved</i> OMB No. 0704-0188	
<p>The public reporting burden for this collection of information is estimated to average 1 hour per response, including the time for reviewing instructions, searching existing data sources, gathering and maintaining the data needed, and completing and reviewing the collection of information. Send comments regarding this burden estimate or any other aspect of this collection of information, including suggestions for reducing this burden, to Department of Defense, Washington Headquarters Services, Directorate for Information Operations and Reports (0704-0188), 1215 Jefferson Davis Highway, Suite 1204, Arlington, VA 22202-4302. Respondents should be aware that notwithstanding any other provision of law, no person shall be subject to any penalty for failing to comply with a collection of information if it does not display a currently valid OMB control number. PLEASE DO NOT RETURN YOUR FORM TO THE ABOVE ADDRESS.</p>					
1. REPORT DATE (DD-MM-YY) November 2011		2. REPORT TYPE Technical Paper		3. DATES COVERED (From - To) 1 November 2011 – 1 November 2011	
4. TITLE AND SUBTITLE FATIGUE CRACK DETECTION VIA LOAD-DIFFERENTIAL GUIDED WAVE METHODS (PREPRINT)				5a. CONTRACT NUMBER FA8650-09-C-5206	
				5b. GRANT NUMBER	
				5c. PROGRAM ELEMENT NUMBER 62102F	
6. AUTHOR(S) Jennifer E. Michaels, Sang Jun Lee, Xin Chen, and Thomas E. Michaels				5d. PROJECT NUMBER 4349	
				5e. TASK NUMBER 41	
				5f. WORK UNIT NUMBER LP106300	
7. PERFORMING ORGANIZATION NAME(S) AND ADDRESS(ES) Georgia Tech Research Group 305 10th Street NW Atlanta, GA 30332				8. PERFORMING ORGANIZATION REPORT NUMBER	
9. SPONSORING/MONITORING AGENCY NAME(S) AND ADDRESS(ES) Air Force Research Laboratory Materials and Manufacturing Directorate Wright-Patterson Air Force Base, OH 45433-7750 Air Force Materiel Command United States Air Force				10. SPONSORING/MONITORING AGENCY ACRONYM(S) AFRL/RXLP	
				11. SPONSORING/MONITORING AGENCY REPORT NUMBER(S) AFRL-RX-WP-TP-2011-4362	
12. DISTRIBUTION/AVAILABILITY STATEMENT Approved for public release; distribution unlimited.					
13. SUPPLEMENTARY NOTES This work was funded in whole or in part by Department of the Air Force contract FA8650-09-C-5206. The U.S. Government has for itself and others acting on its behalf an unlimited, paid-up, nonexclusive, irrevocable worldwide license to use, modify, reproduce, release, perform, display, or disclose the work by or on behalf of the U.S. Government. PA Case Number and clearance date: 88ABW-2011-4533, 19Aug 2011. Preprint journal article to be submitted to Review of Progress in Quantitative NDE Conference Proceeding. This document contains color.					
14. ABSTRACT Detection of fatigue cracks originating from fastener holes is an important application for structural health monitoring (SHM) of civil, mechanical and aerospace structures, but their detection via ultrasonic guided waves can be problematic when cracks are tightly closed in the absence of applied tensile loads. Proposed here are load-differential guided wave methods, which compare signals at one load to those at another load at the same damage state. The main advantage of such methods is that cracks can be detected and localized by analyzing current signals obtained from different loading conditions without using baseline data from the damage-free state. The efficacy of the proposed load-differential methods is examined using fatigue test data where multiple cracks grow from a single through-hole. Data were acquired with a spatially distributed array of piezoelectric discs by recording ultrasonic signals as a function of applied uniaxial load at intervals through the fatigue test.					
15. SUBJECT TERMS fatigue cracks, guided waves, load-differential imaging, structural health monitoring					
16. SECURITY CLASSIFICATION OF:			17. LIMITATION OF ABSTRACT: SAR	18. NUMBER OF PAGES 10	19a. NAME OF RESPONSIBLE PERSON (Monitor) Charlie Buynak
a. REPORT Unclassified	b. ABSTRACT Unclassified	c. THIS PAGE Unclassified			

FATIGUE CRACK DETECTION VIA LOAD-DIFFERENTIAL GUIDED WAVE METHODS

Sang Jun Lee, Jennifer E. Michaels, Xin Chen, and Thomas E. Michaels

School of Electrical and Computer Engineering, Georgia Institute of Technology,
Atlanta, GA 30332-0250

ABSTRACT. Detection of fatigue cracks originating from fastener holes is an important application for structural health monitoring (SHM) of civil, mechanical and aerospace structures, but their detection via ultrasonic guided waves can be problematic when cracks are tightly closed in the absence of applied tensile loads. Proposed here are load-differential guided wave methods, which compare signals at one load to those at another load at the same damage state. The main advantage of such methods is that cracks can be detected and localized by analyzing current signals obtained from different loading conditions without using baseline data from the damage-free state. The efficacy of the proposed load-differential methods is examined using fatigue test data where multiple cracks grow from a single through-hole. Data were acquired with a spatially distributed array of piezoelectric discs by recording ultrasonic signals as a function of applied uniaxial load at intervals through the fatigue test. Load-differential guided wave images are generated from residual signals via delay-and-sum imaging methods, and these images are evaluated in terms of their ability to detect and localize fatigue cracks.

Keywords: Fatigue cracks, Guided Waves, Load-differential Imaging, Structural Health Monitoring
PACS: 43.35.Cg, 43.35.Ty, 43.35.Zc, 43.40.Qi, 43.60-c

INTRODUCTION

Guided waves (e.g., Lamb waves) have been considered for many SHM applications because of their ability to travel long distances and maintain sensitivity to damage [1]. One conventional approach to detect damage is to compare *in situ* signals to baselines recorded from the undamaged structure. By comparing current signals to damage-free baselines, signal changes caused by structural damage can be tracked [2,3]. Such methods can handle some structural complexity, but have unwanted sensitivity to variations in environmental and operational conditions (e.g., temperatures and loads), which can cause high false alarm rates. On the other hand, baseline-free methods analyze current signals without comparison to damage-free baselines; such methods are inherently less sensitive to environmental and operational variations.

In this paper, we consider varying applied tensile static loads such as arise during normal operation of a structure. The effects of such loads on propagation of both bulk and guided ultrasonic waves in homogeneous media are generally well understood [4,5]. Even

though the effects of applied loads may be unavoidable in the *in situ* environment and significantly affect the ultrasonic signals by changing both structural dimensions and wave speeds [6], applied loads can also improve damage detectability when the tensile load is large enough to open a tight crack. Here, we propose load differential imaging, which generates a series of images from differences in sparse array signals caused by small static loading variations. The efficacy of the proposed method in detecting and locating fatigue cracks is demonstrated from fatigue tests of an aluminum plate having six surface-bonded piezoelectric discs.

DATA ANALYSIS

Data analysis is a two-step process consisting of chirp filtering followed by imaging. Both steps are described here.

Chirp Filtering

The theory of the chirp filtering is presented in detail in our previous work [7] and is reviewed here. Lamb waves in a plate may be generated by a linear chirp source, $s_c(t)$, where the frequency is swept from a minimum value to a maximum value over a fixed time interval. The Fourier transform of $s_c(t)$ is $S_c(\omega)$, where ω is the angular frequency. Let $h(t)$ be the impulse response associated with specific transmitter and receiver locations, which includes both the structural response (Green's function) and all transducer and instrumentation effects. Note that $H(\omega)$ is the Fourier transform of $h(t)$. Since the system is assumed to be linear, the response to the chirp excitation can be expressed in the frequency domain as,

$$R_c(\omega) = H(\omega)S_c(\omega). \quad (1)$$

Now consider a different excitation, such as a tone burst, given by $s_d(t)$. In the frequency domain we have,

$$R_d(\omega) = H(\omega)S_d(\omega). \quad (2)$$

The response to the signal $s_d(t)$ can be readily calculated from the measured chirp response by division in the frequency domain,

$$R_d(\omega) = R_c(\omega)G(\omega) \text{ where } G(\omega) = \frac{S_d(\omega)}{S_c(\omega)}. \quad (3)$$

The filter $G(\omega)$ can be readily constructed from the known Fourier transforms of the chirp excitation and the desired excitation when the bandwidth of the desired excitation is within that of the chirp excitation. Finally, $R_d(\omega)$ is transformed back to the time domain to obtain the tone burst response signal.

Imaging Method

The imaging method used here is based upon the signal changes between two measurements, and is thus a differential method. Consider sets of signals recorded from all possible pairs of a sparse array under two different conditions. For example, the different conditions may be damage state, as is typical, or loads, as is considered here. For convenience, we refer to the first set as baseline signals and to the second set as current signals; note that the term "baseline" does not necessarily mean "damage-free." A set of residual signals is calculated by subtracting the baseline signals from the current signals. These residual signals are analyzed via delay-and-sum imaging whereby they are back

propagated and summed at each pixel location using an appropriate delay law [3], and the pixel intensity is computed as the square of the summed values:

$$E(x, y) = \left[\sum_{i=1}^{N-1} \sum_{j=i+1}^N s_{ij}(t_{ij}(x, y)) \right]^2. \quad (4)$$

In this equation $s_{ij}(t)$ is the residual signal from transducer pair ij , and t_{ij} is the delay time that corresponds to the time of propagation from the transmitter to the pixel location to the receiver. If the i th transducer (the transmitter) is located at (x_i, y_i) , the j th transducer (the receiver) is located at (x_j, y_j) , and the pixel location is (x, y) , then t_{ij} is,

$$t_{ij}(x, y) = \frac{\sqrt{(x_i - x)^2 + (y_i - y)^2} + \sqrt{(x_j - x)^2 + (y_j - y)^2}}{c_g}, \quad (5)$$

where c_g is the group velocity. Although the residual signal in Eq. (4) can be either the raw (RF) signal, or the envelope-detected (rectified) signal, here we consider only the envelope-detected signals. The group velocity is estimated from the times of the first arrivals from all transducer pairs.

EXPERIMENTS

Experimental Setup

An aluminum plate specimen was instrumented with an array of six piezoelectric discs and subjected to cyclic loading to investigate loading effects on guided wave propagation. A 6061 aluminum plate of 305 mm \times 610 mm \times 3.18 mm was machined to enable mounting in an MTS machine as shown in Figure 1. The transducers were fabricated from 7 mm diameter, 300 kHz, radial mode PZT discs that were attached to the plate with epoxy and further protected with a backing of bubble-filled epoxy.

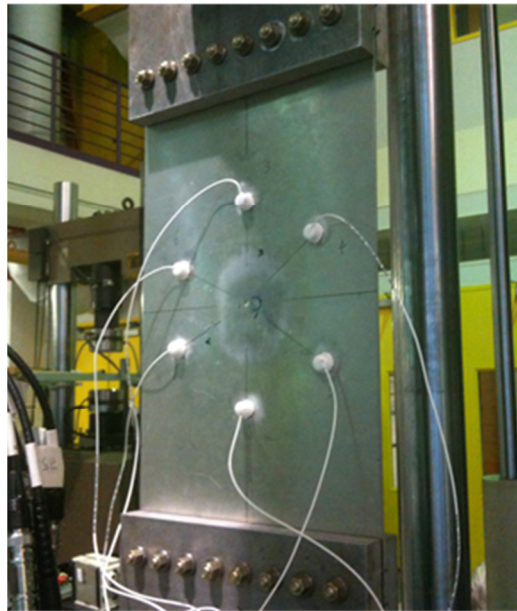


FIGURE 1. Aluminum specimen (thickness of 3.18 mm) with attached PZT transducers. Note that the uniaxial loads were applied in the vertical direction.

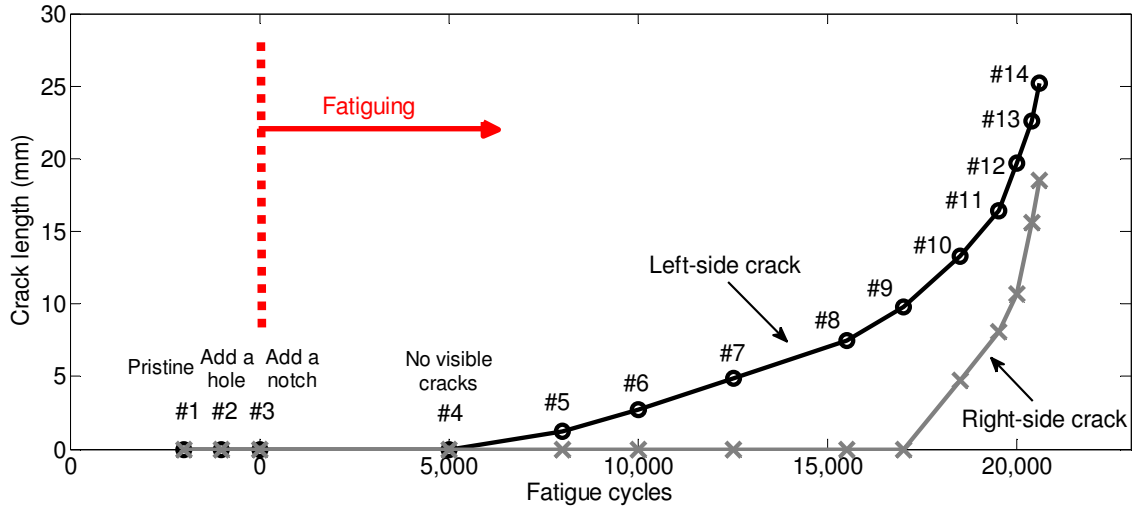


FIGURE 2. Growth curves of two fatigue cracks. Note that “#xx” stands for the dataset number.

An arbitrary waveform generator applied a ± 10 V, 50–500 kHz linear chirp excitation to the transducers, and signals were digitized with a 20 MHz sampling rate and a 14-bit resolution. Twenty waveforms were averaged for each acquisition to improve the signal-to-noise ratio. Using Eq. (3), the signals measured from the chirp excitation were filtered to obtain the equivalent responses to a 5-cycle tone burst excitation at 100 kHz, where the A_0 guided wave mode was dominant.

The specimen was fatigued with a 3 Hz sinusoidal tension-tension loading profile from 16.5 to 165 MPa. Fatiguing was periodically paused to record ultrasonic data as a function of applied tensile load from 0 MPa to 115 MPa in steps of 11.5 MPa, resulting in a total of 11 static loading conditions for each data set. After the first dataset was recorded from the pristine plate (i.e. before fatiguing), a 5.1 mm diameter through hole was drilled in the center of the specimen. A small starter notch was subsequently made on one side of the hole to act as a site for initiation of a fatigue crack. Data were recorded as summarized in Figure 2, where crack lengths were measured with a scale under an applied load. Fatiguing was continued until the largest crack reached about 25 mm in length.

Load-Differential Signals

Here, we consider the effects of applied loads on recorded signals and not using any previously obtained “damage-free” baseline signals. Figure 3(a) shows signals from transducer pair 2-5 (i.e., transmitting on 2 and receiving on 5) as a function of load when the specimen is pristine (i.e. no damage/hole/notch). The shape of the signals does not change significantly with load. To more clearly see signal changes with load, Figure 3(b) shows differential signals where each signal is the difference of two signals recorded at adjacent loads (e.g., 40% minus 30%). As expected, when there is no damage, all the signals are similar and the corresponding differential signals are similar as well even though the applied loads increase. Even when there are fatigue cracks, the raw signals look similar as shown in Figure 3(c). However, Figure 3(d) clearly shows that there is an initial large change in the first arrival of the first differential signal as the crack on one side of the hole opens up and blocks the direct wave. At about 70% load (the 7th differential signal from the bottom), it appears that the crack on the other side of the hole opens up.

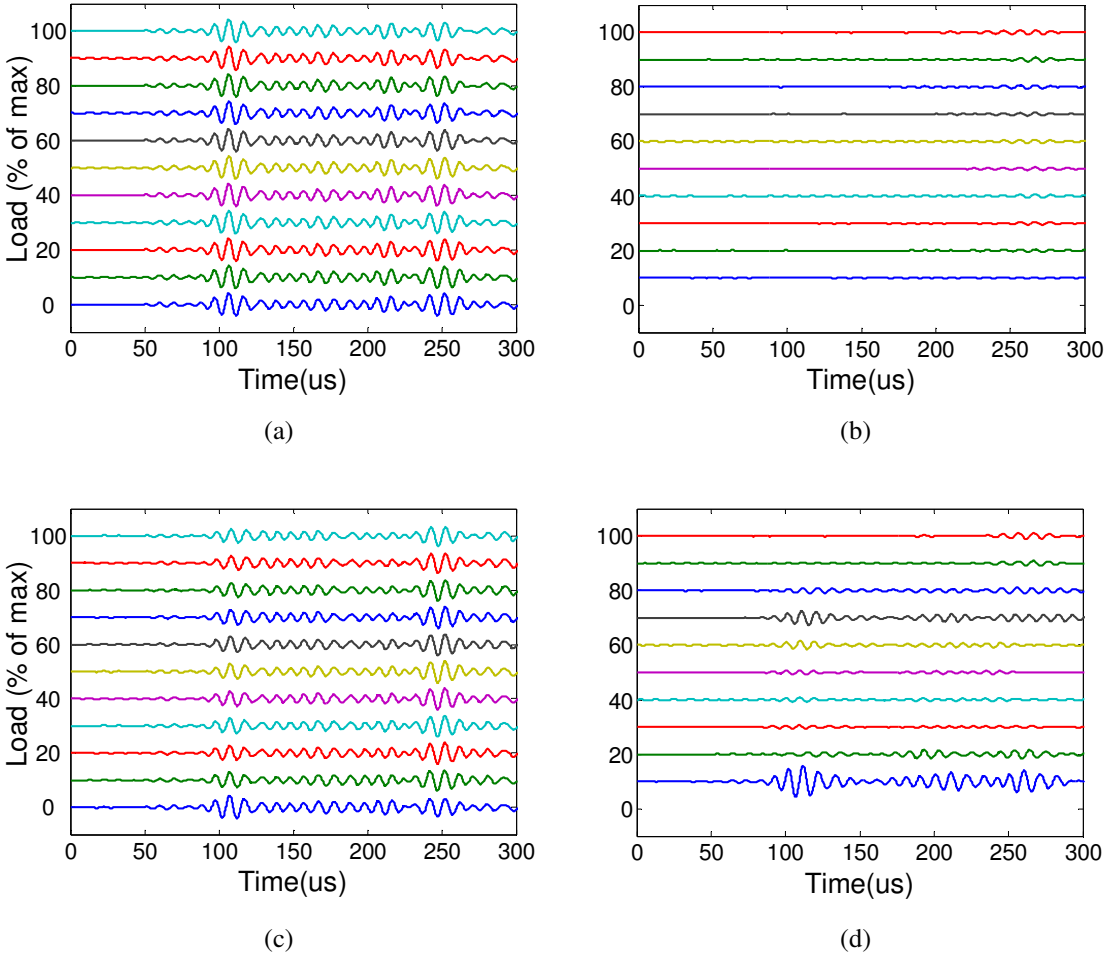


FIGURE 3. (a) Signals recorded from transducer pair 2-5 of dataset 3 as a function of applied load. (b) Corresponding differential signals as a function of applied load, where the vertical scale is four times that of Figure 3(a). (c) Signals recorded from transducer pair 2-5 of dataset 10 as a function of applied load. (d) Corresponding differential signals as a function of applied load.

Impacts of Loads on Damage-Free Baseline Imaging

Here, the effects of loads on imaging using damage-free baselines are examined by generating several images from various loading conditions. The previously described imaging method is applied by comparing current signals to damage-free baselines. Four different images were obtained and analyzed by comparing datasets 3 (baseline signals) and 7 (current signals) where the primary difference between these two datasets is a single fatigue crack that is about 5 mm in length. Figures 4(a) and (b) show the resulting images from two mismatched loading cases. The fatigue crack cannot be detected and localized effectively from these images because Figure 4(a) has only the artifacts around the edges and Figure 4(b) shows some indication of the fatigue crack around the center hole but with comparable artifacts. Next, Figures 4(c) and (d) show the resulting images from two matched loading cases. In particular, the fatigue crack is still invisible in Figure 4(c) (zero loads) because the crack is tightly closed, whereas Figure 4(d) clearly shows the existence of the fatigue crack because the applied load opens the crack for the current signals of dataset 7. This observation implies that the fatigue crack can be effectively imaged only when applied loads are both well-matched between current signals and baselines, and sufficiently large to open the crack.

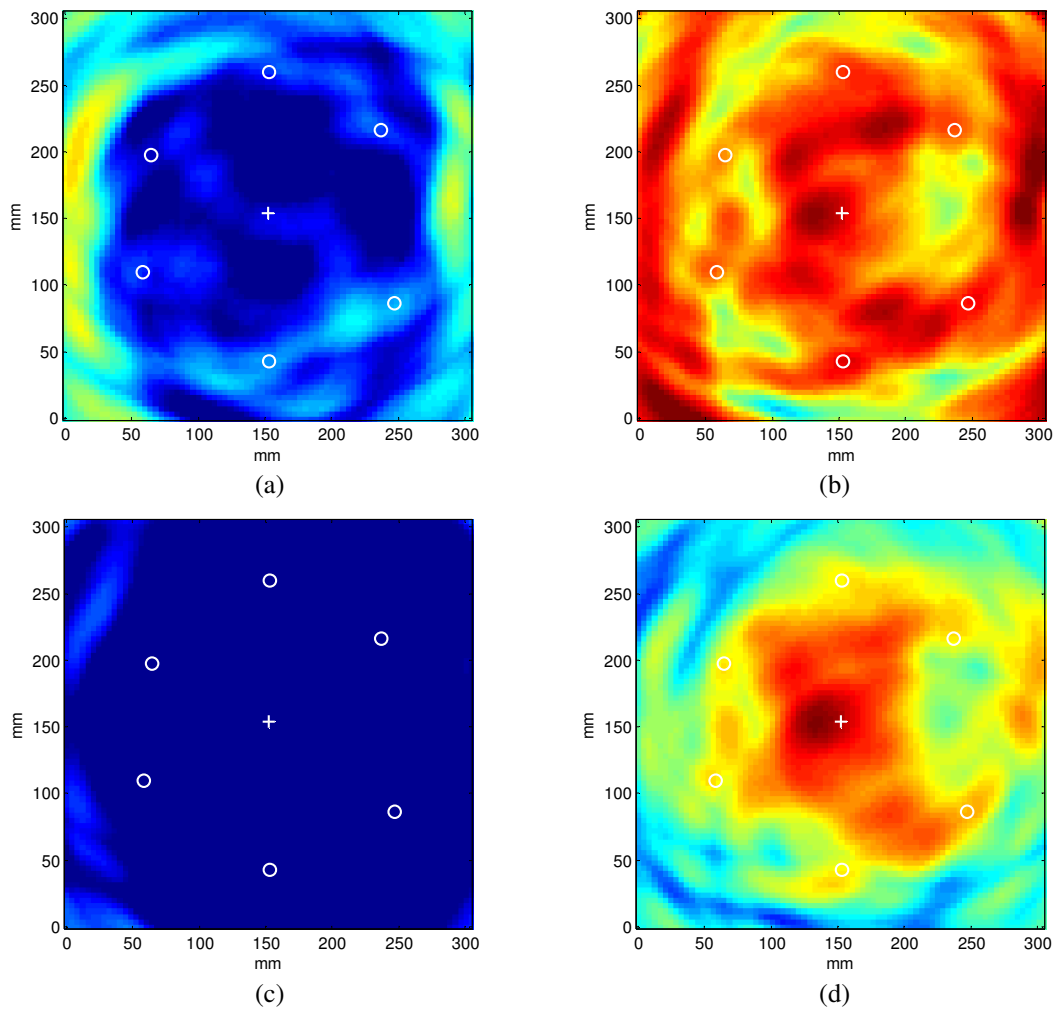
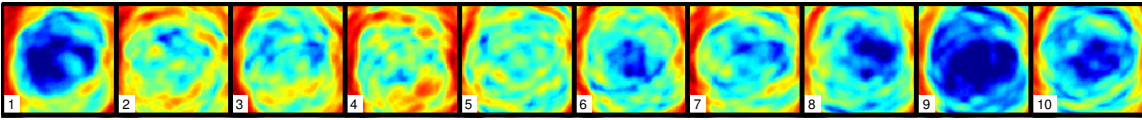


FIGURE 4. Images constructed between dataset 3 (baseline signals) and dataset 7 (current signals) from various loading conditions. (a) 115 MPa/0 MPa, (b) 0 MPa/115 MPa, (c) 0 MPa/0 MPa, and (c) 115 MPa/115 MPa. All four images are shown on the same 10 dB color scale.

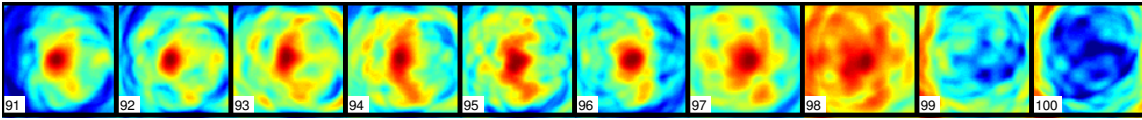
These imaging results show a clear advantage of imaging fatigue cracks in the presence of applied loads: the ability of loads to open cracks. This advantage holds regardless of other structural complexity such as fastener holes or notches. However, if loads are too small, cracks may be tightly closed and thus undetectable. The minimum amplitude of the required load to open the crack depends on its size, with smaller, tighter cracks requiring larger loads to open.

Load-differential Imaging

The results of the previous section motivate a new approach to imaging of fatigue cracks referred to as the load-differential imaging method. In this method the “baseline signals” are recorded at one load, and the “current signals” are recorded at the same damage state but at a slightly increased tensile load (10% increment of the maximum load in this study). The difference between the signals is thus caused by a combination of crack opening effects and loading effects for certain loading combinations.

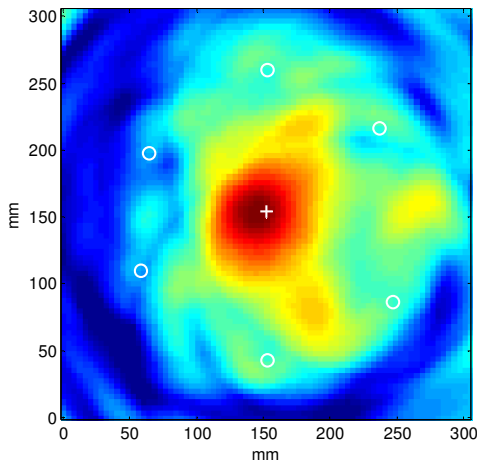


(a)

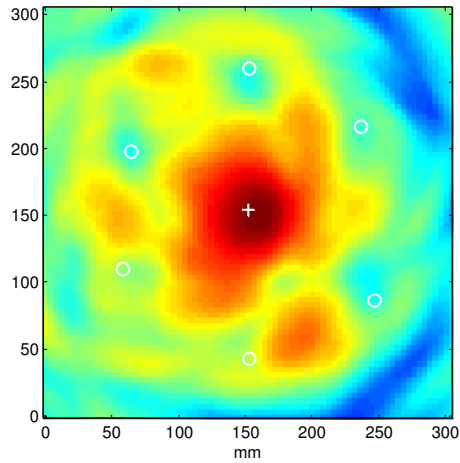


(b)

FIGURE 5. Two series of the load-differential images plotted on a 10 dB scale normalized to the peak of each image. (a) Dataset #1 (no damage). (b) Dataset #10 (two cracks).



(a)



(b)

FIGURE 6. Two load-differential images from dataset 10, plotted on a 10 dB scale normalized to the peak of each image. (a) 0 MPa/11.5 MPa. (b) 57.5 MPa/69 MPa.

Figure 5 shows two series of ten load-differential images from datasets 1 and 10 to validate this idea. The difference in loads is 11.5 MPa for each image, and the baseline loads start at 0 MPa and increment by 11.5 MPa. Figure 5(a) only shows image artifacts around the edges, but Figure 5(b) clearly indicates the possible existence of the fatigue cracks from most of the images. In particular, Figure 6(a), which is the first load-differential image of dataset 10, shows the existence of one fatigue crack on the left side of the hole and Figure 6(b), which is the seventh load-differential image of dataset 10, shows the existence of the second crack on the right side of the hole. These results indicate that the proposed load-differential imaging method has the potential to detect multiple cracks from the load-dependent behavior of crack opening.

CONCLUSIONS

This study has proposed and demonstrated a load-differential imaging method for detecting and locating fatigue cracks via guided waves. The measured ultrasonic signals show that an applied tensile load can open a crack, where the loading amplitude depends on its size. The images generated from the load-differential signals clearly show the

initiation and progression of fatigue crack growth without using any previously obtained damage-free baseline signals. Also, load-differential imaging has the potential for imaging multiple cracks that have different load responses. Discrimination of fatigue cracks from other load-induced effects such as fastener contact variations should be a topic of future work that considers more complex structures.

ACKNOWLEDGEMENTS

This work is sponsored by the Air Force Research Laboratory under Contract No. FA8650-09-C-5206 (Charles Buynak, Program Manager).

REFERENCES

1. D. E. Adams, *Health Monitoring of Structural Materials and Components: Methods with Applications*, John Wiley & Sons, West Sussex, 2007, ch. 1.
2. C. Wang, J. Rose, and F.-K. Chang, "A synthetic time-reversal imaging method for structural health monitoring," *Smart Mater. Struct.*, **13**, pp. 415–423 (2004).
3. J. E. Michaels, "Detection, localization and characterization of damage in plates with an *in situ* array of spatially distributed ultrasonic sensors," *Smart Mater. Struct.*, **17**, 035035 (15pp) (2008).
4. Y.-H. Pao and U. Gamer, "Acoustoelastic waves in orthotropic media," *J. Acoust. Soc. Am.*, **77**, pp. 806-812 (1985).
5. N. Gandhi, J. E. Michaels and S. J. Lee, "Acoustoelastic Lamb wave propagation in a homogeneous, isotropic aluminum plate," in *Review of Progress in QNDE*, **30A**, edited by D. O. Thompson and D. E. Chimenti, AIP Conference Proceedings vol. 1335, American Institute of Physics, Melville, NY (2011), pp. 161-168.
6. S. J. Lee, N. Gandhi, J. E. Michaels, and T. E. Michaels, "Comparison of the Effects of Applied Loads and Temperature Variations on Guided Wave Propagation," in *Review of Progress in QNDE*, **30A**, edited by D. O. Thompson and D. E. Chimenti, AIP Conference Proceedings vol. 1335, American Institute of Physics, Melville, NY (2011), pp. 175-182.
7. J. E. Michaels, S. J. Lee, J. S. Hall and T. E. Michaels, "Multi-mode and multi-frequency guided wave imaging via chirp excitations," in *Proc. SPIE*, **7984**, edited by T. Kundu, (2011), 79840I (11 pp) .